Cell. Mol. Life Sci. 64 (2007) 1571 – 1582
1420-682X/07/121571-12
DOI 10.1007/s00018-007-7031-0

Cellular and Molecular Life Sciences

Research Article

Conformational changes in a bacterial multidrug transporter are phosphatidylethanolamine-dependent

B. Gbaguidi, P. Hakizimana, G. Vandenbussche and J.-M. Ruysschaert*

Laboratory for Structure and Function of Biological Membranes, Structural Biology and Bioinformatics Center, Free University of Brussels, CP206/2, Bd du Triomphe, 1050 Brussels (Belgium), Fax: +32 26 50 53 82, e-mail: jmruyss@ulb.ac.be

Received 23 January 2007; received after revision 2 April 2007; accepted 20 April 2007
Online First 25 May 2007

Abstract. LmrP is an electrogenic H^+/drug antiporter that extrudes a broad spectrum of antibiotics. Five carboxylic residues are implicated in drug binding (Asp142 and Glu327) and proton motive force-mediated restructuring (Asp68, Asp128 and Asp235). ATR-FTIR (Attenuated Total Reflection – Fourier Transform Infrared) and tryptophan quenching experiments revealed that phosphatidylethanolamine (PE) is required to generate the structural intermediates induced by ionization of carboxylic residues. Surprisingly, no ionization-induced conformational changes were detectable in the absence of PE, suggesting either that carboxylic acid residues do not ionize or that ionization does not lead to any conformational change. The mean pKa of carboxylic residues evaluated by ATR-FTIR spectroscopy was 6.5 for LmrP reconstituted in PE liposomes, whereas the pKa calculated in the absence of PE was 4.6. Considering that 16 of the 19 carboxylic residues are located in the extramembrane loops, the pKa values obtained in the absence and in the presence of PE suggest that the interaction of the loop acid residues with the membrane interface depends on the lipid composition.

Keywords. Secondary transporter, LmrP, conformational change, PE-environment, multidrug transporter.

Introduction

One of the multidrug resistance extrusion systems of *Lactococcus lactis* is the proton motive force-driven secondary transporter LmrP, a 408-amino acid protein with 12 putative transmembrane helices [1] (Fig. 1) capable of extruding a large variety of lipophilic cationic compounds including ethidium, daunomycin, tetraphenylphosphonium, Hoechst 33342 [2] and antibiotics [3]. Mutagenesis studies have allowed the identification of several carboxylic acidic residues involved in LmrP-mediated proton/substrate antiport [4]. D68, D128 and D235 residues contribute to the conformational changes observed in response to a proton gradient, and D142 and D327 are involved in the conformational changes observed in response to substrate binding [5]. Based on crystal structures obtained for lactose permease (LacY) end EmrE [6, 7], the translocation pathways of the proton/substrate transporter are thought to open (outward-facing conformation) and close (inward-facing conformation) in respond to proton gradient- and substrate binding-induced conformational changes. These conformational changes may be brought about by the protonation/ deprotonation of acidic residues that have been shown to be functionally important [8]. pH

* Corresponding author.

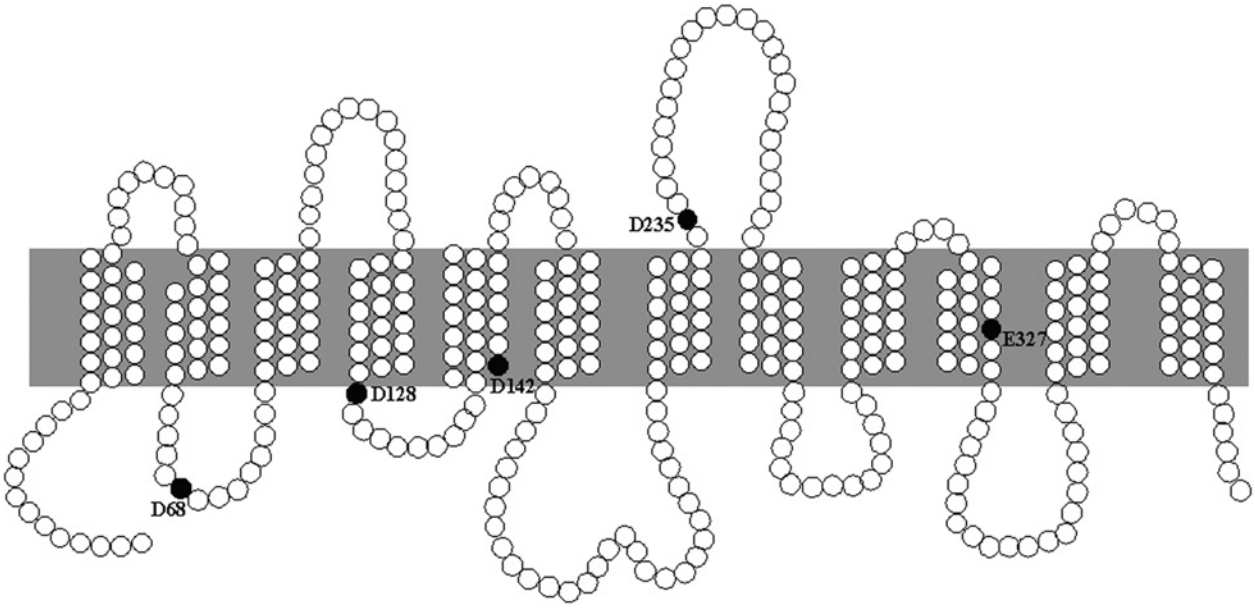

Figure 1. Topology of LmrP protein. Carboxylic acid residues D142 and E327 are involved in substrate binding, and residues D68, D128 and D235 are involved in restructuring induced by the proton gradient.

changes will act on a small set of amino acid side chains and trigger a conformational change [9].

On the other hand, the topology, folding and function of secondary transporters are PE-dependent, as illustrated for LacY [10–13], GabP [14] and PheP [15]. Topology studies of LacY performed on *Escherichia coli* and proteoliposomes have revealed an inverted topology of the N-terminal six-transmembrane helical bundle in membrane bilayers lacking PE, while assembly of the C-terminal helical bundle was correct. Addition of PE restored native topology and sugar transport activity, highlighting the dynamic dependence of secondary transporters on lipid composition for their topology and activity. Interestingly, such topological changes were also observed for LacY reconstituted into proteoliposomes, suggesting that cellular protein assembly machinery was not involved in the observed changes [13].

Although considerable progress has been made in our understanding of the effects of lipid composition on the membrane topology and function of secondary transporters, the precise structural changes involved in these processes have not been satisfactorily described. In the present work, LmrP and mutants (cytosolic D128C and D235C and membrane D142C and E327C) were overexpressed in *L. lactis*, purified and reconstituted in proteoliposomes [4, 5]. To determine whether the ionization of these acidic residues is involved in structural changes associated with substrate/proton translocation, we monitored tryptophan residue accessibility to hydrophilic (acrylamide) and hydrophobic (TEMPO) quenchers and the accessibility of amide protons in the presence/absence of PE at pH 5.5, 6.5 and 7.5. ATR-FTIR was used to evaluate the pKa values associated to the carboxylic residues in the presence or absence of PE.

Materials and methods

Materials. Ni^{2+}-nitrilotriacetic acid (Ni-NTA)-agarose was from Qiagen. *E. coli* phosphatidylethanolamine (PE), *E. coli* phosphatidylglycerol (PG) and *E. coli* cardiolipin (CL) were from Avanti Polar Lipids, and phosphatidylcholine (PC; egg yolk) was obtained from Sigma-Aldrich. Dodecyl-β-D-maltoside (DDM) was from Across organics. Triton X-100, 2,2,6,6-Tetramethyl-1-piperidinyloxyl (TEMPO) and valinomycin were obtained from Sigma-Aldrich. Acrylamide came from Merck, the phospholipids dosage kit was from Roche and Hoechst 33342 was obtained from Molecular Probes.

Bacterial strains and growth conditions. *L. lactis* NZ9000 [16] was used in combination with the NICE system [17] for overexpression of LmrP wild type (WT) and D128C, D142C, E327C and D235C mutants [4, 18, 19]. *L. lactis* cells were grown at 30°C in M17 medium (Difco) supplemented with 0.5 % w/v glucose and 5 μg/mL chloramphenicol. Expression of LmrP variants was induced by adding approximately 10 ng nisin A per mL at an A_{660} of about 0.6, and cells were harvested 120 min after induction.

Mass spectrometry. The mass spectra were acquired on a Q-Tof Ultima mass spectrometer (Waters/Micromass, Milford, USA), equipped with a Z-spray nanoelectrospray source and operating in the positive and negative ion modes. The total lipid extract was loaded into gold-palladium-coated borosilicate nanoelectrospray capillaries (Proxeon, Odense, Denmark). Capillary voltages of 1.1–1.5 kV and a cone voltage of 50 V were typically used. The source temperature was held at 80°C. Data acquisition was performed using a MassLynx 4.0 system. The spectra represent the combination of 1-s scans. For the collision-induced dissociation (CID) measurements, the precursor ions were selected in the quadrupole and collided with argon in the hexapole collision cell using an appropriate collision energy (typically 20–40 eV).

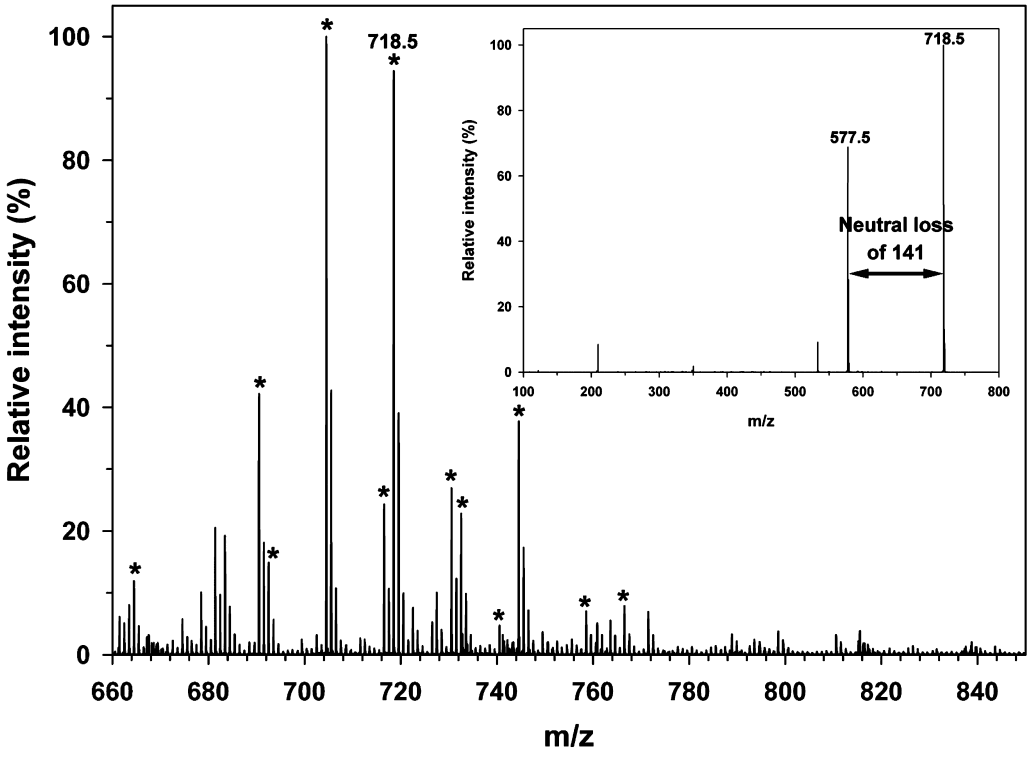

Figure 2. Mass spectrum of the *Lactococcus lactis* total lipid extract in the positive ion mode. The insert represents, as an example, the collision-induced dissociation of the precursor $[M+H]^+$ at 718.5 Th. The fragmentation was characterized by a neutral loss of 141, corresponding to loss of the ethanolaminephosphate head group [41]. The peaks presenting the same characteristic fragmentation pattern are indicated by an asterisk.

Purification and reconstitution of LmrP. His-tagged WT and mutated LmrP were purified by affinity chromatography using Ni-NTA-agarose as described [20]. Briefly, solubilized membrane proteins were mixed with Ni-NTA resin (~25 µL resin/mg protein), which was equilibrated with 50 mM potassium phosphate (pH 8.0) supplemented with 100 mM NaCl, 10% v/v glycerol, 0.05% detergent (DDM) (buffer A) and 10 mM imidazole, followed by gentle shaking for 60 min at 4°C. The resin was transferred to a Bio-spin column (Bio-Rad) and subsequently washed with 20 column volumes buffer A and 10 mM imidazole and 10 column volumes buffer A and 20 mM imidazole. The protein was eluted with buffer A (pH 7.0) containing 250 mM imidazole, and 500-µL fractions were collected.

A dried film of 1.5 mg phospholipids (67% PE/23% PG/10% CL or 67% PC/23% PG/10% CL) was obtained by evaporation of chloroform under a flow of nitrogen, followed by overnight drying under vacuum. Liposomes were prepared by sonication of the lipid film for 5–8 min on a 250W Vibra Cell Sonifier in 2.7 mL 10 mM Tris pH 7.4, 0.5 mM EDTA, 1 mM DTT, 75 mM NaCl. DDM was added to the sonicated lipid suspension in a 1:2 w/w lipid/detergent ratio. The purified LmrP protein was mixed with the detergent-saturated liposomes at a protein to lipid ratio of 1:10 w/w and incubated for 30 min at room temperature under gentle agitation. The detergent was then removed by absorption on SM2 Bio-Beads (three incubations of 2 h under continuous stirring in the presence of 80 mg Bio-Beads). In order to demonstrate the association of proteins with lipids, the supernatant collected from the Bio-Beads mixed with an equal volume of 80% sucrose was overlaid with a 30 to 5% sucrose linear gradient and centrifuged overnight at 120 000 × *g* at 4°C in a Beckman L7 ultracentrifuge with a SW60 rotor. The gradient was fractionated, and phospholipid and protein distributions along the gradient were determined by enzymatic colorimetric assays (Phospholipids Dosage Kit from Roche) of the PC and tryptophan fluorescence, respectively. PC was added to the liposome preparation in a 3:1 w/w PE 67%/PG 23%/CL 10% or PC 67%/PG 23%/CL 10% to PC ratio. In order to eliminate the sucrose, the fractions containing the proteoliposomes were washed twice by centrifugation in 3 mM Hepes pH 7.4 for 2 h at 150 000 × *g* and then resuspended in ~20 µL of the same buffer.

Imposition of a ΔpH across LmrP-containing liposomes. To impose an artificial proton gradient (ΔpH), proteoliposomes were collected by centrifugation (18 000 × *g* for 30 min at 4°C), resuspended in 20 mM potassium phosphate (pH 7.0) supplemented with 100 mM potassium acetate and 2 mM $MgSO_4$ (buffer I, final pH 7.8) and frozen in liquid nitrogen. The frozen proteoliposomes were thawed at room temperature, collected by centrifugation (18 000 × *g* for 30 min at 4°C) and resuspended to a final concentration of 0.5 mg protein/mL in buffer I. A 10-µL sample was diluted 100-fold into 20 mM potassium phosphate (pH 7.0) containing 50 mM K_2SO_4, 2 mM $MgSO_4$ (buffer II, final pH 6.9) and 0.5 µM valinomycin to collapse the electrical potential.

The ΔpH across the proteoliposomal membranes was monitored by measuring the pH-sensitive fluorescence of pyranine [21]. Pyranine was added to buffer I at a final concentration of 0.5 mM and encapsulated into liposomes during the freeze-thawing steps described above to generate the ΔpH. External pyranine was removed by extensive washing of the proteoliposomes. The internal pH was followed by measuring the pyranine fluorescence (excitation at 461±4 nm, emission 511±4 nm) after dilution of 10 µL proteoliposomes into buffer II. Fluorescence after complete dissipation of ΔpH was determined by addition of 0.5% Triton X-100 into the liposome suspension. A correlation between pyranine fluorescence and pH was made by measuring the fluorescence of pyranine in buffers at pH values ranging between 6.9 and 7.8.

Hoechst 33342 transport in proteoliposomes. Hoechst 33342 transport carried out with proteoliposomes containing about 10 µg WT and mutated LmrP was driven by an imposed ΔpH, as

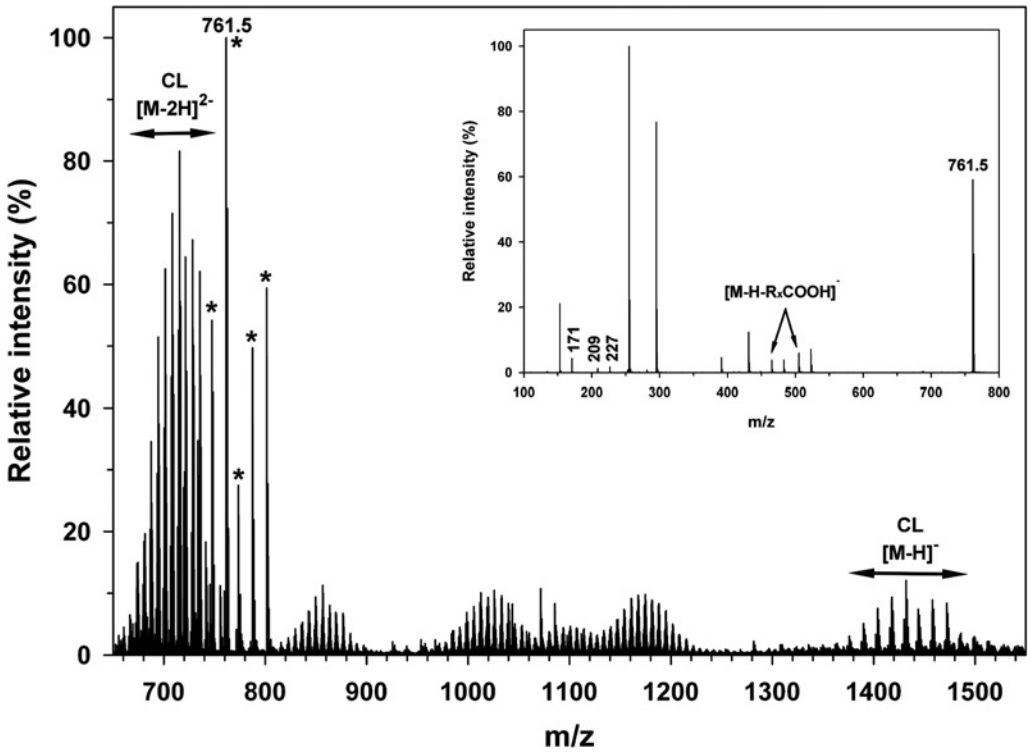

Figure 3. Mass spectrum of the *Lactococcus lactis* total lipid extract in the negative ion mode. The insert represents, as an example, the collision-induced dissociation of the precursor $[M-H]^-$ at 761.5 Th. The fragmentation pattern was characteristic of phosphatidylglycerols with peaks at 227 Th, corresponding to combined losses of sn-1 and sn-2 acyl chains as a ketene and an acid, at 209 Th corresponding to combined losses of the acids at sn-1 and sn-2, and 171 Th corresponding to the glycerol phosphate anion [42]. Identification of phosphatidylglycerols was also confirmed from peaks arising from neutral loss of free fatty acid substituents indicated as $[M-H-R_xCOO]^-$ in the spectrum. The peaks presenting the same characteristic fragmentation pattern are indicated by an asterisk. A similar fragmentation profile allowed us to identify cardiolipins (CL) in the spectrum.

explained previously. Hoechst 33342 was added at a final concentration of 1 μM to the liposome suspension. The fluorescence was monitored on a SLM Aminco 8000 fluorimeter using excitation and emission wavelengths of 355 and 457 nm, respectively.

Tryptophan fluorescence quenching by acrylamide and TEMPO. Quenching experiments were carried out with hydrophobic (TEMPO) and hydrophilic (acrylamide) quenchers on an SLM Aminco 8000 fluorimeter at an excitation wavelength of 290 nm to reduce the absorbance of acrylamide. Fluorescence intensities were measured at 333 nm after addition of 5 μL quencher. Quenching data were analysed according to the Stern-Volmer equation for collisional quenching:

$F_0/F = 1 + K[Q]$, where F_0 and F are the fluorescence intensities in the absence and presence of quencher, [Q] is the molar concentration of quencher and K is the Stern-Volmer quenching constant. Data were subjected to a linear fit up to 100 mM acrylamide or 5 mM TEMPO. Stern-Volmer constants were plotted as a function of the pH imposed.

Attenuated Total Reflection-Fourier transform infrared spectroscopy (ATR-FTIR). ATR-FTIR spectra were recorded at room temperature on a Bruker IFS55 FTIR spectrophotometer equipped with a liquid nitrogen-cooled mercury-cadmium-telluride detector at a nominal resolution of 2 cm^{-1} and encoded every 1 cm^{-1}. The spectrophotometer was continuously purged with air dried on a FTIR purge gas generator 75–62 Balston (Maidstone, UK) at a flow rate of 5.8 L/min. The internal reflection element (ATR) was a germanium plate (50 × 20 × 2 mm) with an aperture angle of 45°, yielding 25 internal reflections [22].

Sample preparation. The sample contained 20 μg LmrP reconstituted in the presence/absence of PE. Thin films of oriented multilayers were obtained by slowly evaporating the sample on one side of the ATR plate under a stream of nitrogen [23]. The ATR plate was then sealed in a universal sample holder.

Hydrogen/deuterium exchange kinetics. The 20-μg sample of reconstituted LmrP was deposited on a germanium plate as described above. Nitrogen was saturated with D_2O by bubbling in a series of three vials containing D_2O. Before starting the deuteration, ten spectra of the sample were recorded to test the stability of the measurements. At time zero, the D_2O-saturated N_2 flux, at a flow rate of 100 mL/min, was connected to the sample. For each kinetic time point, 24 scans were recorded and averaged at a resolution of 2 cm^{-1}. The signal from the atmospheric water was subtracted as described by Goormaghtigh and Ruysschaert [24]. As described previously [25], deuteration of protein side chains induces modifications in the amide I (1700 to 1600 cm^{-1}) and amide II (1600 to 1500 cm^{-1}) regions. Several parameters modulate their contribution, including the ionization state of the carboxylic amino acids and the fraction of deuterated and undeuterated amino acid side chains for every spectrum of the kinetics. We used homemade software that can compute the contribution of the amino acid side chains as a function of the extent of deuteration [26]. The area of the amide II, characteristic of the δ(N-H) vibration, was obtained by integration between 1596 and 1502 cm^{-1}. For each spectrum, the area of the amide II was divided by the corresponding lipidic ν(C=O) area to take into account small but significant variations in the total intensity due to the presence of D_2O, which induced swelling of the sample layer at the beginning of the kinetics [26]. This ratio expressed in percentage was plotted *versus* deuteration time. The value corresponding to 0 % deuteration is defined by the amide II/lipid ratio obtained before deuteration. The 100 % value corresponds to a zero absorption in the amide II region, observed for full deuteration of the protein.

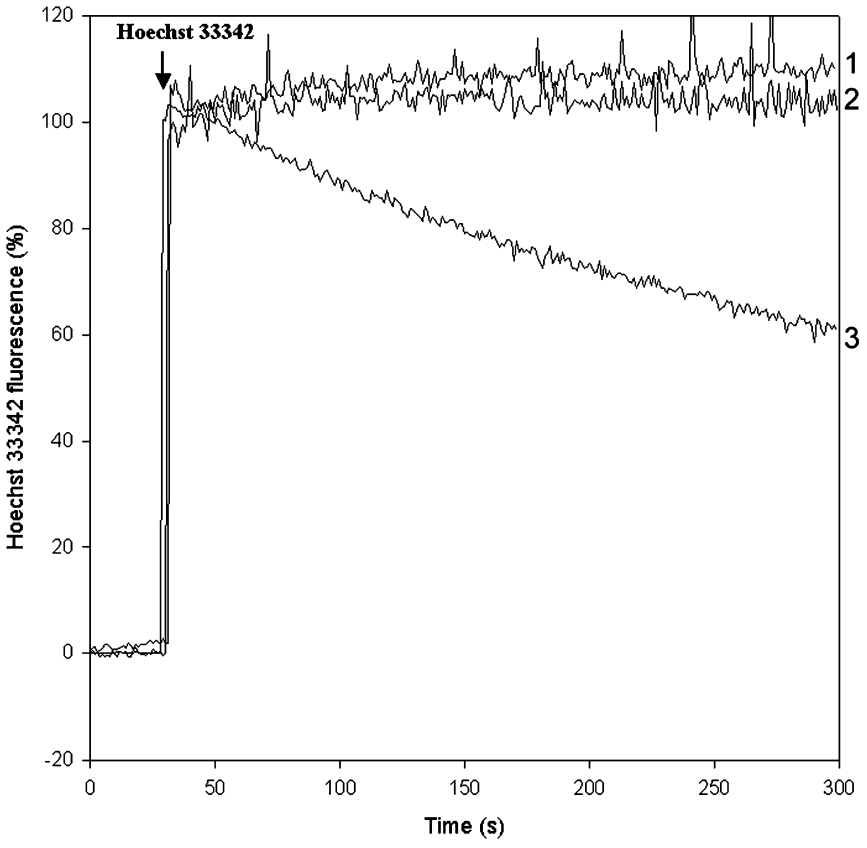

Figure 4. Hoechst 33342 transport in LmrP reconstituted into liposomes. ΔpH across liposomes was imposed as described in Materials and methods. After 30 s of data acquisition (λexc =355 nm and λem =457 nm), 35 μL Hoechst 33342 (100 μM) was added. Fluorescence intensity after addition of Hoechst 33342 was normalized to 100%. Fluorescence was monitored for ~300 s: 1, in the absence of ΔpH; 2, ΔpH (0.9) is imposed to PC-proteoliposomes; 3, ΔpH (0.9) is imposed to PE-containing proteoliposomes.

Flowing buffer in the liquid cell. Buffer solutions or ligand solutions were flowed over the sample using a device previously described [27, 28]. The aforementioned system allows a buffer to flow inside an infrared (IR) liquid cell at the surface of a germanium plate. The geometry of the Internal Reflection Element (IRE) allowed 25 internal reflections. A peristaltic pump adjusted the flow rate to 1.5 mL/min, and a computer-controlled valve selected the buffer. All experiments were performed at 20°C on a Brucker Equinox 55 spectrophotometer equipped with a nitrogen-cooled MCT detector. Reconstituted LmrP (40 μg) was deposited on the germanium plate as described. Buffer A was flowed for 1 h in the cell to obtain a stable IR signal. A first spectrum, referred to as "reference" was recorded in buffer A at a resolution of 2 cm^{-1}. The pump valve was activated to pump in a second buffer, buffer B set at pH (x). Four minutes later, a spectrum (spectrum 2) was recorded, and the valve was switched again to the solution A for 4 min before a third spectrum (spectrum 3) was recorded. Buffer A was 3 mM Mes, 3 mM Hepes pH 7.5; Buffer B was 3 mM Mes, 3 mM Hepes pH x, x decreasing from pH 7.5 to pH 4.5 by steps of 0.5 pH units. The spectra recorded at each pH (x) were subtracted from the "reference" spectrum recorded with a scaling factor set at 1.

Results

Transport activity and substrate affinity of LmrP are lipid-dependent. Figures 2 and 3 show the mass spectrometry patterns of lipids extracted from *L. lactis* as described previously [38]. PE, PG and CL were identified in the positive and negative mode after collision-induced dissociation (CID).

LmrP protein was reconstituted into proteoliposomes (PE 67%/PG 23%/CL 10% or PC 67%/PG 23%/CL 10%). Purified LmrP protein was mixed with detergent-saturated liposomes (lipid to detergent ratio 1:2 w/w) at a protein to lipid ratio of 1:10 w/w. The detergent was removed by adsorption on Bio-Beads [5]. The supernatant collected from the Bio-Beads was loaded on a linear sucrose gradient. Co-migration of lipids and proteins demonstrated that proteoliposomes had been formed (data not shown) for both lipid compositions. PC was added to the liposome preparation in order to evaluate the lipid content.

Hoechst 33342, a fluorescent substrate of LmrP, was used as described previously [5] to monitor LmrP transport activity of PE-proteoliposomes (PE 67%/PG 23%/CL 10%) and PC-proteoliposomes (PC 67%/PG 23%/CL 10%). Active extrusion of Hoechst required a pH gradient imposed across PE-containing liposomes. LmrP did not transport Hoechst after replacement of PE with PC (Fig. 4). Proteoliposomes made of CL and PG did not show any LmrP transport activity, even though a pH gradient was maintained across the lipid bilayer (data not shown).

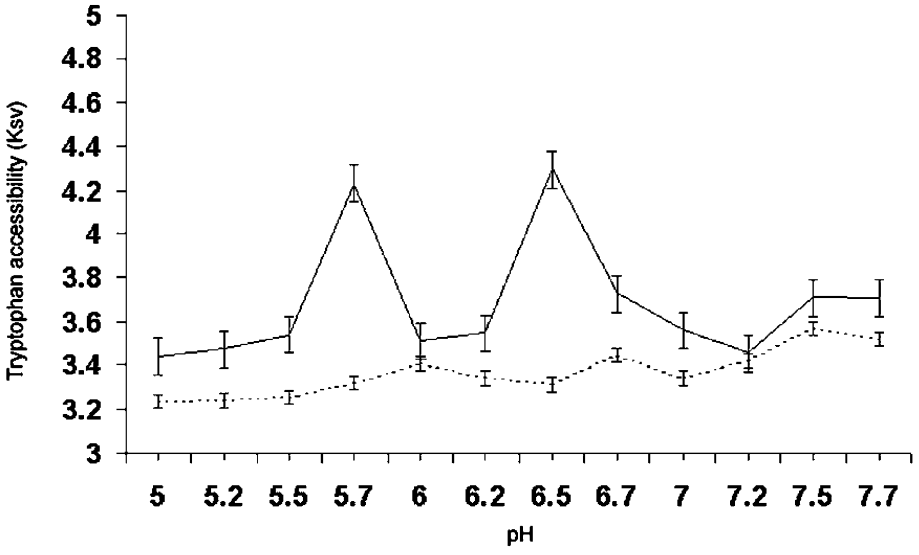

Figure 5. Membrane tryptophan residue accessibility to the hydrophobic quencher TEMPO. The Stern-Volmer constant Ksv is plotted as a function of the pH for LmrP reconstituted in the presence (solid line) or in the absence (dotted line) of PE. The curves represent the means of at least three experiments.

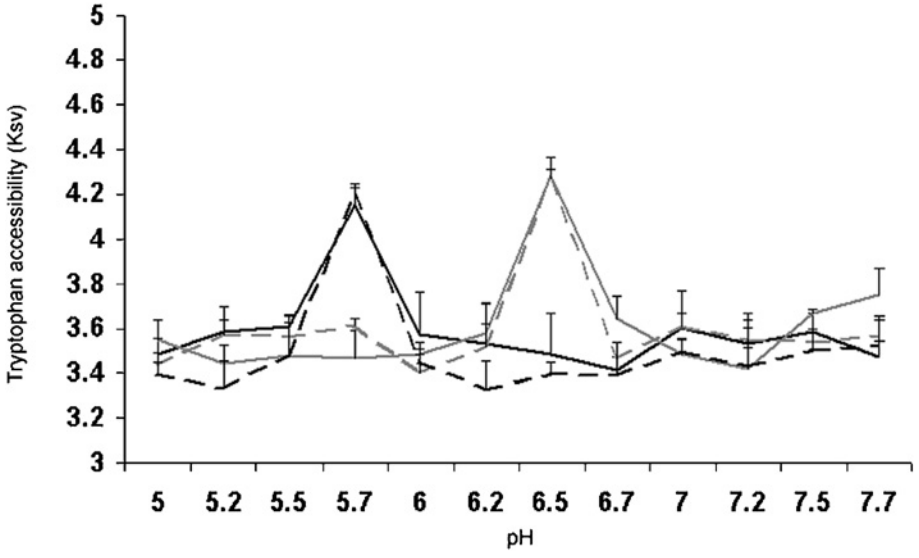

Figure 6. Membrane tryptophan residue accessibility to the hydrophobic quencher TEMPO. The Stern-Volmer constant Ksv is plotted as a function of the pH for LmrP mutants reconstituted in the presence of PE: D128C, gray solid line; D142C, gray dotted line; D235C, black solid line and E327C, black dotted line. The curves represent the means of at least three experiments.

Conformational changes induced by ionization of LmrP carboxylic acid residues are lipid-dependent.

Tryptophan fluorescence quenching. Acidic residues involved in proton motive force mediated-restructuring and drug binding have been identified [4, 5, 19]. To investigate whether the ionization of these acidic residues is involved in substrate/proton translocation and can modify LmrP conformation, we monitored tryptophan residue accessibility to hydrophilic (acrylamide) and hydrophobic (TEMPO) quenchers at different pH, ranging from 5 to 8. Acrylamide was added first in order to quench hydrophilic tryptophan residues. After the last addition of acrylamide, no fluorescence change was detectable. TEMPO was then added to quench transmembrane tryptophan residues [29]. The accessibility of membrane tryptophan residues (Stern-Volmer constant) plotted as a function of pH values was maximal at pH 5.7 and 6.5 (Fig. 5). The E327C mutation located in the transmembrane domains and the D235C mutation located in the cytosolic domains abolished the peak observed at pH 6.5, suggesting that modification of their ionization states is responsible for the conformational change at pH 6.5 (Fig. 6). The Asp142 mutation located in transmembrane domains and the Asp128 mutation located in cytosolic domains abolished the peak observed at pH 5.7, suggesting that modification of their ionization states is responsible for the conformational change observed at pH 5.7 (Fig. 6). Proteoliposomes lacking PE did not show changes in tryptophan accessibility at different pH (Fig. 5), suggesting that either ionization of carboxylic acid residues did not occur or ionization changes of

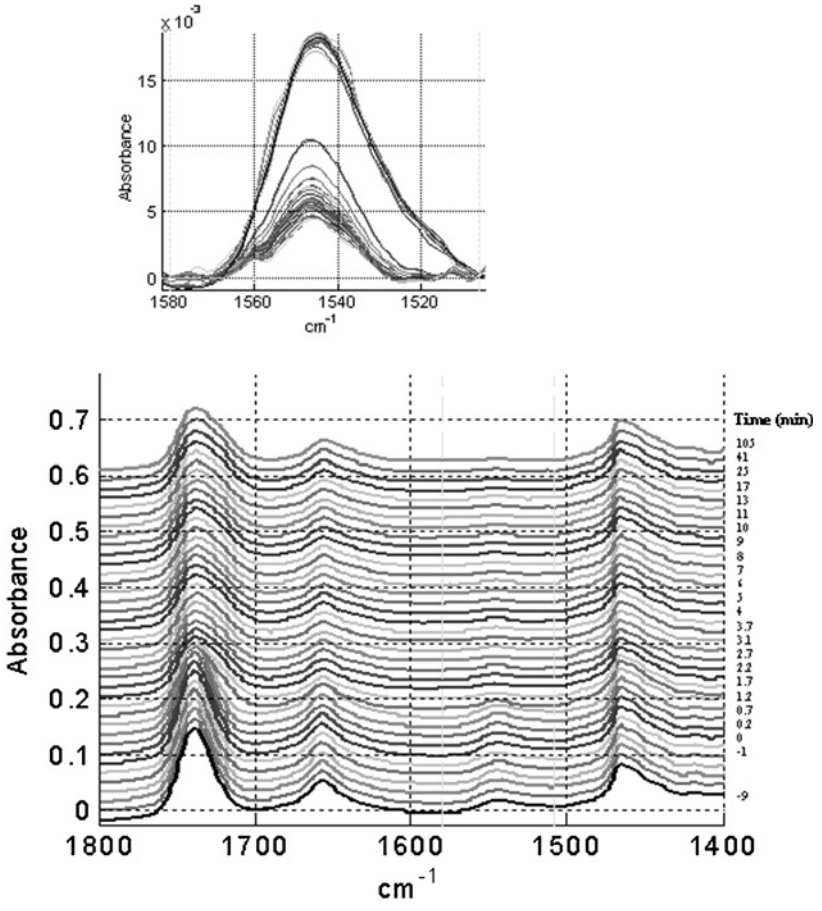

Figure 7. Infrared spectra in the 1800 to 1400 cm^{-1} region of LmrP actively reconstituted into lipids. Thin films were obtained by slowly evaporating a sample containing 20 μg LmrP on an attenuated total reflection element. Spectra were recorded as a function of the time (in minutes) of exposure to D_2O-saturated N_2. Negative times refer to spectra recorded before starting the deuteration procedure. The inset shows the decrease in intensity of the amide II band during the H/D exchange kinetics of LmrP.

carboxylic acid residues did not lead to any LmrP conformational change.

Accessibility of amide protons. At constant experimental conditions (pH and temperature), the rate of hydrogen/deuterium exchange is related to solvent accessibility to the NH amide groups of the protein. Changes in H/D exchange rates reflect changes in the tertiary structure of the proteins and/or stability of a specific conformational state. Infrared spectroscopy allows exclusive monitoring of the exchange rate of the amide protons and has been applied to detect tertiary structural changes in membrane proteins [30–33]. Amide hydrogen exchange is followed by monitoring the decrease in the amide II absorption peak (maximum at 1554 cm^{-1}) as a function of the time of exposure to D_2O-saturated N2 (Fig. 7). The decreasing area of amide II between 100 and 0% is reported in Fig. 8. The decrease in the amide II peak (1554 cm^{-1}) is proportional to the number of hydrogens that have been exchanged with deuterium. H/D exchange measurements were performed on LmrP reconstituted in the presence/absence of PE at pH 5.5, 6.5 and 7.5.

For LmrP reconstituted in the absence of PE, the exchange rate at pH 7.5 (2 pH units) is 88-fold higher than at pH 5.5 (Fig. 9 and Table 1), a value very close to the rate expected in the absence of any conformational change. Indeed, for each pH unit in the absence of any structural change, the rate of exchange is multiplied by a factor approaching 10 [23]. We previously verified that this pH dependence is identical for proteins in solution or deposited on an IR reflection element [23]. The exchange rate of LmrP reconstituted in the presence of PE was only 2-fold higher at pH 5.5 (very far away from the expected factor 100). The H/D exchange rate was 250-fold higher at pH 6.5 than at pH 5.5. Altogether, these data convincingly confirm the conformational changes revealed by tryptophan quenching at pH 5.5 and pH 6.5 for LmrP reconstituted in the presence of PE and the absence of conformational change in the absence of PE.

The pKa of LmrP carboxylic residues is PE-dependent. LmrP contains 19 carboxylic residues (10 Glu and 9 Asp) located mainly in cytosolic loops. IR spectra provide direct information about the ionization states of carboxylic residues [$\upsilon(COO^-)$ at 1575 cm^{-1} and $\upsilon(COOH)$ at 1730 cm^{-1}] [28]. In our experimental setup, a sealed chamber in contact with the sample deposited on a germanium plate

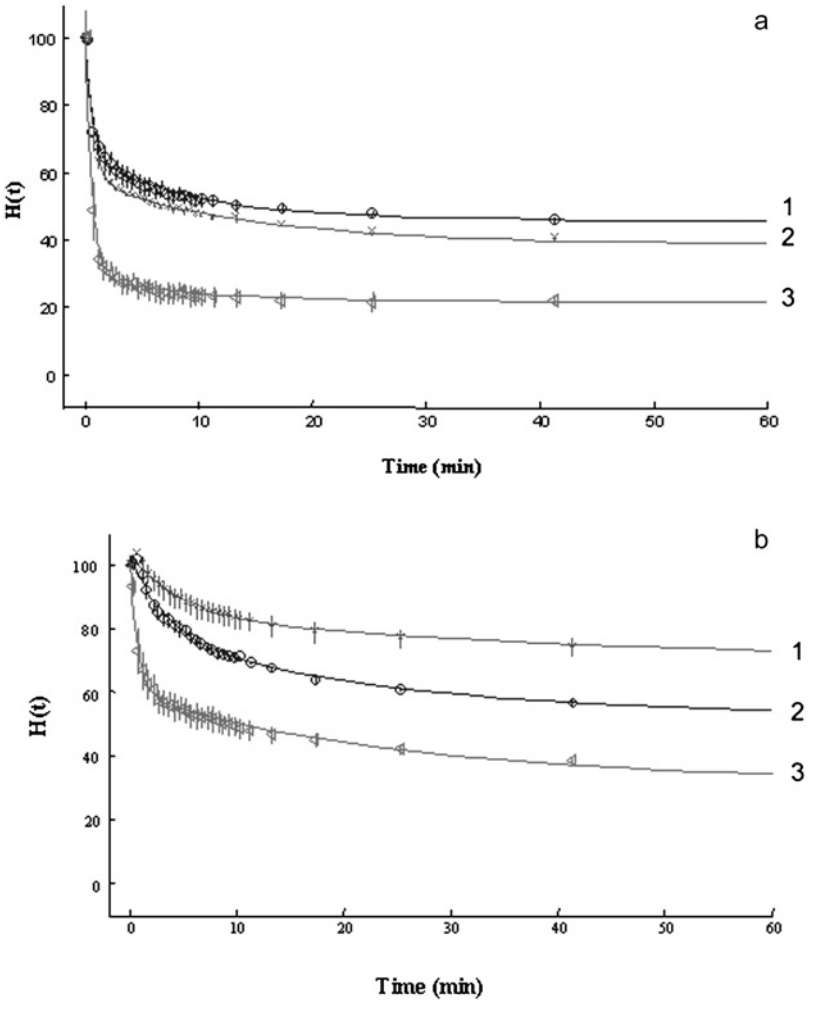

Figure 8. The evolution of the proportion of exchanged amide bonds was computed between 0 and 100% as a function of the deuteration time. Deuteration kinetics of LmrP reconstituted (*a*) with PE at pH 5.5 (1), pH 7.5 (2) or pH 6.5 (3) and without PE (*b*) at pH 5.5 (1), pH 6.5 (2) or pH 7.5 (3).

Table 1. H/D exchange factors (K).

K PE-proteoliposomes		K PC-proteoliposomes	
1	pH 5.5	1	pH 5.5
250	pH 6.5	7	pH 6.5
2.4	pH 7.5	88	pH 7.5

H/D exchange factors (K) were computed (Fig. 9) using the least squares method in order to obtain the best overlapping between pH 5.5, 6.5 and 7.5 curves. An arbitrary value of 1 corresponds to the exchange rate at pH 5.5.

was flushed with buffer solutions at different pH, ranging from 7.5 to 4.5 by steps of 0.5 units, at a flow rate of 1.5 mL/min. A first spectrum was recorded at pH 7.5 and is referred to as "sample reference state". A second spectrum was recorded at pH x, with x ranging from 7.5 to 4.5 by steps of 0.5 units. A third spectrum was recorded again at pH 7.5, and then a new cycle started. The difference between the first spectrum and the second spectrum allows visualization of the effect of pH x on carboxylic residue ionization states (Fig. 10). A titration curve was drawn by plotting the integrated COO^- peak area as a function of pH (Fig. 11). The mean pKa value of carboxylic residues was 6.5 for LmrP reconstituted in the presence of PE and 4.6 in the absence of PE. High pKa values have been reported for membrane-embedded acidic residues in LacY [34]. A value of 4.6 is rather representative of a water environment.

Discussion

Monitoring of tryptophan residue accessibility of LmrP reconstituted in the presence of PE (for pH values ranging from 5 to 8) revealed that drastic changes in accessibility occur at pH 5.7 and pH 6.5. The fact that mutation of either Asp128 (cytosolic residue) or Asp142 (membrane residue) abolished the conformational change monitored at pH 5.7 suggests that these residues are located in structural domains that might interact with each other. The same mechanism might explain the pH-induced

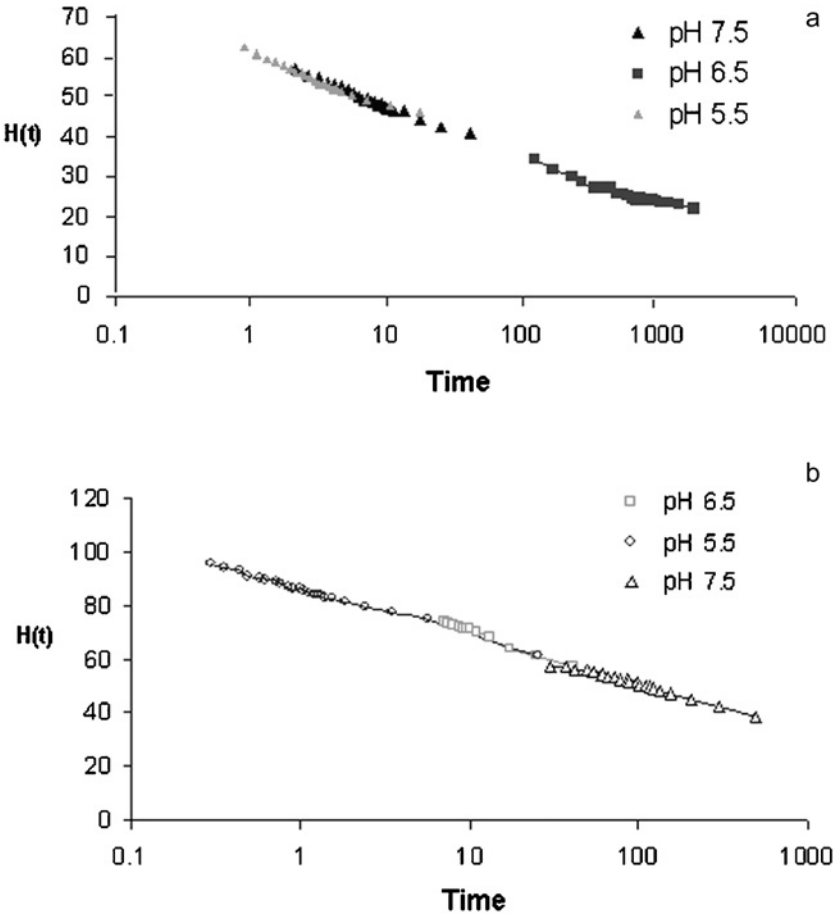

Figure 9. Percentage of non-exchanged amide hydrogens H(t) as a function of log (t). The time scale was multiplied by an appropriated factor (K) (Table 1) in other to obtain the best overlap between two successive curves, using the pH 5.5 curve as a reference. LmrP reconstituted (*a*) with PE and (*b*) without PE.

structural change associated to residues Asp235 (cytosolic residue) and Glu327 (membrane residue). Hydrogen/deuterium exchange measurements permitted us to analyse LmrP global structural change at pH 5.5 and pH 6.5. Amide protons were highly accessible at pH 6.5, and 70% were exchanged with deuterium. Since extramembrane residues represent 40% of the protein residues, it is likely that membrane residues are exchangeable at this pH. In contrast, at pH 5.5 only 45% of amide protons were exchanged with deuterium, suggesting that membrane domains were no longer accessible. These pH-dependent modifications of accessibility to the transmembrane domains have been suggested to explain the opened state (outward-facing conformation) and closed state (inward-facing conformation) of the protein during the transport process [9].

LmrP reconstituted into proteoliposomes lacking PE did not show any transport activity. Moreover, its accessibility to the solvent at different pHs revealed that in the absence of PE, LmrP conformation is not influenced by the ionization state of carboxylic acid residues. This points out the fact that the formation of structural intermediates during the transport process is lipid-dependent and that the cytosolic carboxylic residues can either interact with positively charged amino acid residues or with the positively charged polar head of PE, which is less accessible in PC where three methyl groups surround the positive charge; preliminary data (not shown) support the latter hypothesis. Substitution of PE with monomethyl- or dimethyl-PE did not modify transport activity and amide proton accessibility, whereas addition of a third methyl group drastically affected both transport and accessibility (data not shown). Mean pKa values of carboxylic acid residues were estimated in the presence or absence of PE. A value of 4.6 observed in the absence of PE suggests that cytosolic loops are distant from the membrane interface and are mainly located in an aqueous medium. The higher pKa value of LmrP carboxylic residues measured in the presence of PE might be a consequence of their tighter interaction with lipid membrane, where PE is a major component. Radresa et al. [28] obtained a mean apparent pKa of 6 for H^+/ATPase acidic residues. In the case of bacteriorhodopsin, high pKa

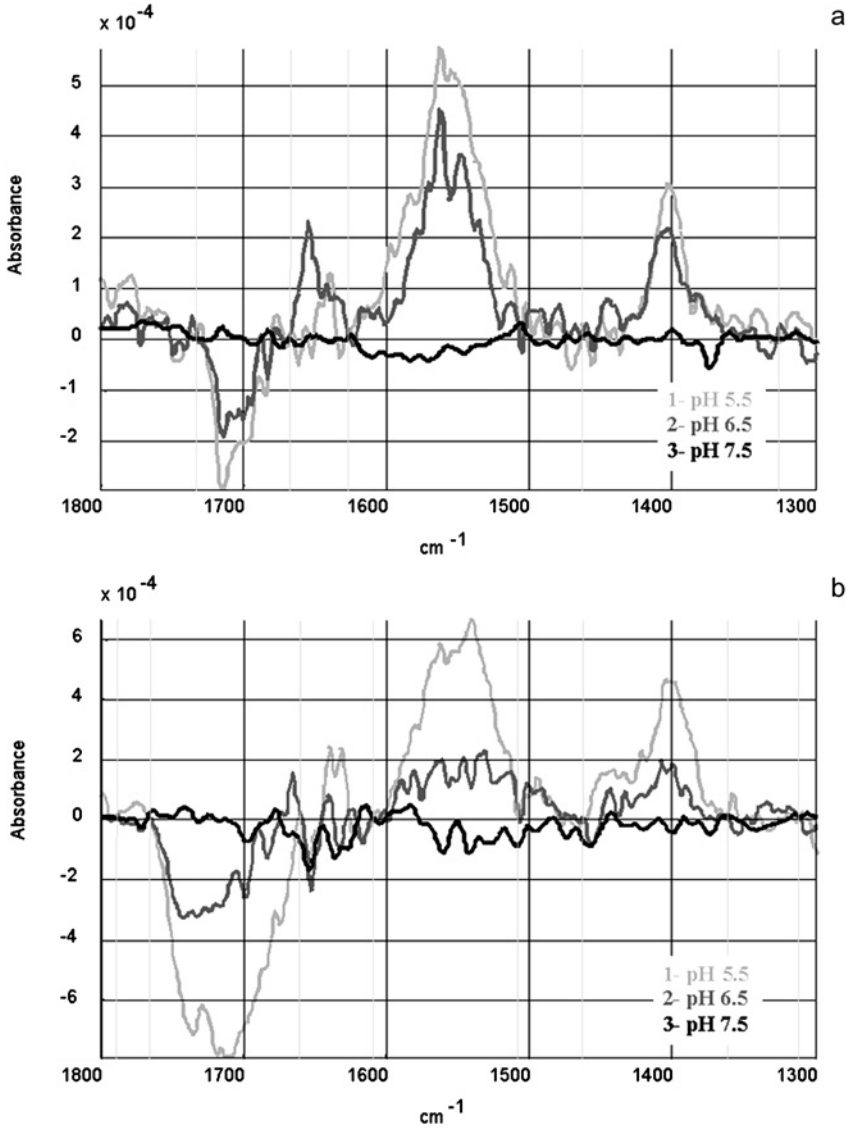

Figure 10. Ionization state of LmrP reconstituted in the presence (*a*) or absence (*b*) of PE. Every FTIR spectrum was recorded at pH x (x ranging from 7.5 to 4.5 by step of 0.5 pH units) and subtracted from the "reference spectrum" at pH 7.5. FTIR difference spectra are shown for pH 7.5, 6.5 and 5.5. The vibration bands of ionized carboxylic residues (COO^-) and protonated residues (COOH) peak at 1575 cm^{-1} and 1730 cm^{-1}, respectively.

values were reported for membrane-embedded carboxylic residues [35, 36]. In the case of LmrA, a multidrug transporter expressed in *L. lactis* bacteria, E314, a carboxylic residue that plays a key role in the conformation coupling between ATP binding/hydrolysis at the nucleotide-binding domains (NBD) and substrate movement, is present in a hydrophobic microenvironment that elevates its pKa. In a similar way, the pKa of many of the carboxylates responsible for proton translocation by secondary-active transporters have been reported as unusually high [37]. In secondary transporters such as LmrP in which most carboxylic amino acids are located in cytosolic/extramembrane loops, minimal changes in microenvironment at the water/lipid interface can affect ionization states of these residues and make them capable of controlling transport catalytic cycles. Our data suggest that the absence of PE keeps carboxylic residues far away from the membrane/water interface, rendering them incapable of participating in pH-induced conformational changes of LmrP as shown by amide proton accessibility, tryptophan fluorescence quenching and pKa value of acidic residues. In the presence of PE, the cytosolic loops of LmrP are close to the membrane/water interface, keeping carboxylic residues in a position that enables them to participate in pH-induced conformational changes of LmrP. Finally our data demonstrate that PE is required for LmrP activity but do not exclude that other neutral lipids can be involved. High rates of transport activity were observed after *L. lactis* membrane vesicles were fused with PE, but fusing them with PC completely inactivated the transport activity [38]. Others studies have shown that PE and glycolipids are interchangeable: mono-

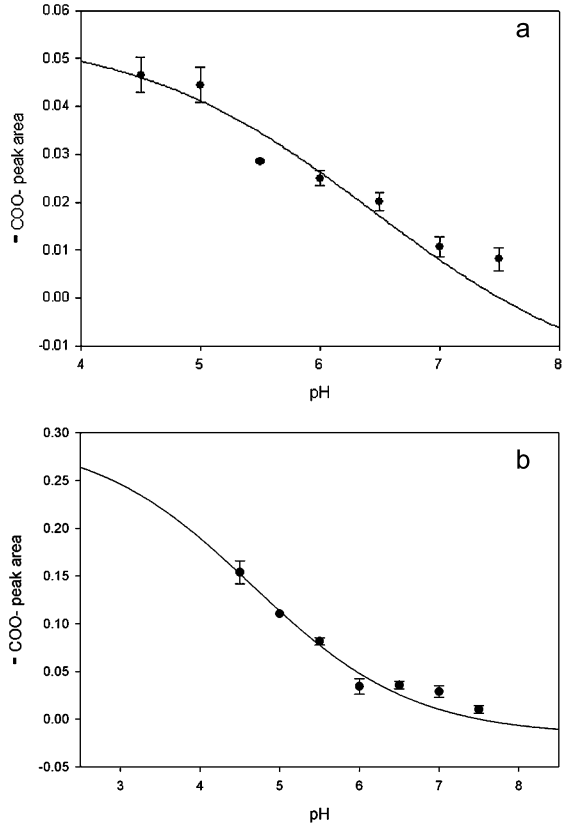

Figure 11. The area of the ν(COO^-) band representative of acidic residue ionization is plotted as a function of pH with PE (*a*) or without PE (*b*). Data were fitted using the Henderson-Hasselbach-derived equation:

$$(COO^- \text{ area}) = \alpha.\frac{10^{(pHx-pKa)}}{1+10^{pHx-pKa}}\ \alpha.\frac{10^{(7.5-pKa)}}{1+10^{7.5-pKa}}$$

where α is a parameter taking account the sample film thickness and the molar coefficient of extinction. (COO^- area) corresponds to the COO^- vibration band area. The mean calculated pKa is 6.5 for LmrP reconstituted in the presence of PE and 4.6 in the absence of PE.

glucosyldiacylglycerol, a foreign lipid, can substitute for PE in essential membrane-associated functions in *E. coli* [39]; and PE and monoglucosyldiacylglycerol are interchangeable in supporting topogenesis and function of the polytopic membrane protein lactose permease [40].

Acknowledgements. We thank Dr. A. Driessen (Groningen) for providing us with the *L. lactis* bacteria strain NZ9000. B. G. is a recipient of financial support from Fonds pour l'Encouragement de la Recherche Scientifique dans l'Industrie et l'Agriculture (Belgium).

References

1 Bolhuis H., Molenaar D., Poelarends G., van Veen H. W., Poolman B., Driessen A. J. and Konings W. N. (1994). Proton motive force-driven and ATP-dependent drug extrusion systems in multidrug-resistant *Lactococcus lactis.* J. Bacteriol. 176, 6957 – 6964.

2 Bolhuis H., Poelarends G., van Veen H. W., Poolman B., Driessen A. J. and Konings W. N. (1995). The Lactococcal lmrP gene encodes a proton motive force-dependent drug transporter. J. Biol. Chem. 270, 26092 – 26098.

3 Putman M., van Veen H. W., Degener J. E. and Konings W. N. (2001) The lactococcal secondary multidrug transporter LmrP confers resistance to lincosamides, macrolides, streptogramins and tetracyclines. Microbiology 147, 2873 – 2880.

4 Mazurkiewicz P., Konings W. N. and Poelarends G. J. (2002) Acidic residues in the lactococcal multidrug efflux pump LmrP play critical roles in transport of lipophilic cationic compounds. J. Biol. Chem. 277, 26081 – 26088.

5 Gbaguidi B., Mazurkiewicz P., Konings W. N., Driessen A. J., Ruysschaert J. M. and Vigano C. (2004) Proton motive force mediates a reorientation of the cytosolic domains of the multidrug transporter LmrP. Cell. Mol. Life Sci. 61, 2646 – 2657.

6 Abramson J., Smirnova I., Kasho V., Verner G., Iwata S. and Kaback H. R. (2003). The lactose permease of *Escherichia coli:* overall structure, the sugar-binding site and the alternating access model for transport. FEBS Lett. 555, 96 – 101.

7 Pornillos O., Chen Y. J., Chen A. P. and Chang G. (2005) X-ray structure of the EmrE multidrug transporter in complex with a substrate. Science 310, 1950 – 1953.

8 Sahin-Toth M., Karlin A. and Kaback H. R. (2000) Unraveling the mechanism of the lactose permease of *Escherichia coli.* Proc. Natl. Acad. Sci. USA 97, 10729 – 10732.

9 Mirza O., Guan L., Verner G., Iwata S., Kaback H. R. (2006) Structural evidence for induced fit and a mechanism for sugar/H^+ symport in LacY. EMBO J. 25, 1177 – 1183.

10 Bogdanov M. and Dowhan W. (1995). Phosphatidylethanolamine is required for *in vivo* function of the membrane-associated lactose permease of *Escherichia coli.* J. Biol. Chem. 270, 732 – 739.

11 Bogdanov M., Sun J., Kaback H. R. and Dowhan W. (1996). A phospholipid acts as a chaperone in assembly of a membrane transport protein. J. Biol. Chem. 271, 11615 – 11618.

12 Bogdanov M. and Dowhan W. (1998). Phospholipid-assisted protein folding: phosphatidy-ethanolamine is required at a late step of the conformational maturation of the polytopic membrane protein lactose permease. EMBO J. 17, 5255 – 5264.

13 Bogdanov M., Heacock P. N. and Dowhan W. (2002) A polytopic membrane protein displays a reversible topology dependent on membrane lipid composition. EMBO J. 21, 2107 – 2116.

14 Zhang W., Campbell H. A., King S. C. and Dowhan W. (2005) Phospholipids as determinants of membrane protein topology. Phosphatidylethanolamine is required for the proper topological organization of the gamma-aminobutyric acid permease (GabP) of *Escherichia coli.* J. Biol Chem. 280, 26032 – 26038.

15 Zhang W., Bogdanov M., Pi J., Pittard J. and Dowhan W. (2003) Reversible topological organization within a polytopic membrane protein is governed by a change in membrane phospholipid composition. J. Biol. Chem. 278, 50128 – 50135.

16 Gajic, O., Buist, G. B., Kojic, M., Topisirovic, L., Kuipers, O. P. and Kok, J. (2003) Novel mechanism of bacteriocin secretion and immunity carried out by lactococcal multidrug resistance proteins. J. Biol. Chem. 278, 34291 – 34298.

17 de Ruyter, P. G., Kuipers, O. P. and de Vos, W. M. (1996) Controlled gene expression systems for *Lactococcus lactis* with the food-grade inducer nisin. Appl. Environ. Microbiol. 62, 3662 – 3667.

18 Putman M., Koole L. A., van Veen H. W. and Konings W. N. (1999) The secondary multidrug transporter LmrP contains multiple drug interaction sites. Biochemistry 38, 13900 – 13905.

19 Mazurkiewicz P., Poelarends G. J., Driessen A. J. and Konings W. N. (2004) Facilitated drug influx by an energy-uncoupled secondary multidrug transporter. J. Biol. Chem. 279, 103 – 108.

20 Putman, M., van Veen, H. W., Poolman, B. and Konings, W. N. (1999) Restrictive use of detergents in the functional recon-

stitution of the secondary multidrug transporter LmrP. Biochemistry 38, 1002 – 1008.
21 Kano K. and Fendler J. H. (1978) Pyranine as a sensitive pH probe for liposome interiors and surfaces. pH gradients across phospholipid vesicles. Biochim. Biophys. Acta 509, 289 – 299.
22 Goormaghtigh E., Cabiaux V. and Ruysschaert J. M. (1990) Secondary structure and dosage of soluble and membrane proteins by attenuated total reflection Fourier-transform infrared spectroscopy on hydrated films. Eur. J. Biochem. 193, 409 – 420.
23 Goormaghtigh E., Raussens V. and Ruysschaert J. M. (1999) Attenuated total reflection infrared spectroscopy of proteins and lipids in biological membranes. Biochim. Biophys. Acta 1422, 105 – 185.
24 Goormaghtigh E., Cabiaux V. and Ruysschaert J. M. (1994) Determination of soluble and membrane protein structure by Fourier transform infrared spectroscopy. II. Experimental aspects, side chain structure, and H/D exchange. Subcell. Biochem. 23, 363 – 403.
25 Krimm S. and Bandekar J. (1986) Vibrational spectroscopy and conformation of peptides, polypeptides, and proteins. Adv. Protein Chem. 38, 181 – 364.
26 Goormaghtigh E., Cabiaux V. and Ruysschaert J. M. (1994) Determination of soluble and membrane protein structure by Fourier transform infrared spectroscopy. III. Secondary structures. Subcell. Biochem. 23, 405 – 450.
27 Scheirlinckx F., Raussens V., Ruysschaert J. M. and Goormaghtigh E. (2004) Conformational changes in gastric H^+/K^+-ATPase monitored by difference Fourier-transform infrared spectroscopy and hydrogen/deuterium exchange. Biochem. J. 382, 121 – 129.
28 Radresa O., Ogata K., Wodak S., Ruysschaert J. M. and Goormaghtigh E. (2002) Modeling the three-dimensional structure of H^+-ATPase of *Neurospora crassa.* Eur. J. Biochem. 269, 5246 – 5258.
29 von Ballmoos C., Appoldt Y., Brunner J., Granier T., Vasella A. and Dimroth P. (2002) Membrane topography of the coupling ion binding site in Na^+-translocating F1F0 ATP synthase. J. Biol. Chem. 277, 3504 – 3510.
30 Vigano C., Manciu L. and Ruysschaert J.-M. (2005) Structure, orientation, and conformational changes in transmembrane domains of multidrug transporters. Acc. Chem. Res. 38, 117 – 126.
31 Vigano, C., Margolles, A, van Veen, H. W., Konings, W. N. and Ruysschaert, J.-M. (2000) Secondary and tertiary structure changes of reconstituted LmrA induced by nucleotide binding or hydrolysis; a Fourier transform attenuated total reflection infrared spectroscopy and tryptophan fluorescence quenching analysis. J. Biol. Chem. 275, 10962 – 10967.
32 Vigano C., Julien M., Carrier I., Gros P. and Ruysschaert J. M. (2002) Structural and functional asymmetry of the nucleotide-binding domains of P-glycoprotein investigated by attenuated total reflection Fourier transform infrared spectroscopy. J. Biol. Chem. 277, 5008 – 5016.
33 Manciu L., Chang X. B., Buyse F., Hou Y. X., Gustot A., Riordan J. R. and Ruysschaert J. M. (2003) Intermediate structural states involved in MRP1-mediated drug transport. Role of glutathione. J. Biol. Chem. 278, 3347 – 3356.
34 Frillingos S. and Kaback H. R. (1996) Monoclonal antibody 4B1 alters the pKa of a carboxylic acid at position 325 (helix X) of the lactose permease of *Escherichia coli.* Biochemistry 35, 10166 – 10171.
35 Dioumaev A. K., Brown L. S., Needleman R. and Lanyi J. K. (1999) Fourier transform infrared spectra of a late intermediate of the bacteriorhodopsin photocycle suggest transient protonation of Asp-212. Biochemistry 38, 10070 – 10078.
36 Zscherp C., Schlesinger R., Tittor J., Oesterhelt D. and Heberle J. (1999) *In situ* determination of transient pKa changes of internal amino acids of bacteriorhodopsin by using time-resolved attenuated total reflection Fourier-transform infrared spectroscopy. Proc. Natl. Acad. Sci. USA 96, 5498 – 5503.
37 Shilling R., Federici L., Walas F., Venter H., Velamakanni S., Woebking B., Balakrishnan L., Luisi B. and Van Veen H. W. (2005) A critical role of a carboxylate in proton conduction by the ATP-binding cassette multidrug transporter LmrA. FASEB J. 19, 1698 – 1700.
38 Driessen A. J., Zheng T., In't Veld G., Op den Kamp J. A. and Konings W. N. (1988) Lipid requirement of the branched-chain amino acid transport system of *Streptococcus cremoris.* Biochemistry 27, 865 – 872.
39 Wikström, M., Xie, J., Bogdanov, M., Mileykovskaya, E., Heacock, P., Wieslander A. and Dowhan, W. (2004) Monoglucosyldiacylglycerol, a foreign lipid, can substitute for phosphatidylethanolamine in essential membrane-associated functions in *Escherichia coli.* J. Biol. Chem. 279, 10484 – 10493.
40 Xie, J., Bogdanov, M., Heacock, P. and Dowhan, W. (2006) Phosphatidylethanolamine and monoglucosyldiacylglycerol are interchangeable in supporting topogenesis and function of the polytopic membrane protein lactose permease. J. Biol. Chem. 281, 19172 – 19178.
41 Pulfer, M. and Murphy, R. C. (2003) Electrospray mass spectrometry of phospholipids. Mass Spectrom. Rev. 22, 332 – 364.
42 Hsu, F.-F. and Turk, J. (2001) Studies on phosphatidylglycerol with triple quadrupole tandem mass spectrometry with electrospray ionization: fragmentation processes and structural characterization. J. Am. Soc. Mass Spectrom. 12, 1036 – 1043.